



Original Articles

Loss of Linc01060 induces pancreatic cancer progression through vinculin-mediated focal adhesion turnover

Xiuhui Shi¹, Xingjun Guo¹, Xu Li^{***}, Min Wang^{**}, Renyi Qin^{*}

Department of Biliary-Pancreatic Surgery, Affiliated Tongji Hospital, Tongji Medical College, Huazhong University of Science and Technology, Wuhan, People's Republic of China

ARTICLE INFO

Keywords:

Pancreatic carcinoma
Long noncoding RNA
FAK
Paxillin

ABSTRACT

There is currently limited knowledge regarding the involvement of long non-coding RNAs (lncRNAs) in cancer development. We aimed to identify lncRNAs with important roles in pancreatic cancer progression. We screened for lncRNAs that were differentially expressed in pancreatic cancer tissues. Among 349 differentially expressed lncRNAs, Linc01060 showed the lowest expression in pancreatic cancer tissues compared with normal pancreatic tissues. Lower Linc01060 expression in pancreatic cancer tissues was significantly associated with a poor prognosis. Linc01060 inhibited pancreatic cancer proliferation and invasion *in vitro* and *in vivo*. Vinculin overexpression inhibited Linc01060-mediated increases in FAK and paxillin phosphorylation, whereas vinculin knockdown reversed the Linc01060-mediated repression of FAK and inactivation of focal adhesion turnover. Vinculin knockdown also accelerated pancreatic cancer cell proliferation by upregulating ERK activity. In biological function analyses, vinculin overexpression abrogated Linc01060-mediated repression of pancreatic cancer cell proliferation and invasion, whereas vinculin counteracted the Linc01060-mediated repression of PC cell proliferation and invasion. These data demonstrate that Linc01060 plays a key role in suppressing pancreatic cancer progression by regulating vinculin expression. These findings suggest that the Linc01060–vinculin–focal adhesion axis is a therapeutic target for pancreatic cancer treatment.

1. Introduction

Pancreatic cancer (PC) is one of the most highly malignant cancers and has a 5-year survival rate of approximately 7% [1,2]. Despite substantial progress in our understanding of PC, there are no effective methods for detecting asymptomatic premalignant or early malignant tumors [3,4]. Furthermore, PC is often diagnosed at an advanced stage because of its deep location and atypical symptoms [5]. Consequently, there is an urgent need to identify novel biomarkers for an early diagnosis, an accurate prognosis, and the development of new therapeutic strategies [6].

Whole-transcriptome analyses have revealed a new class of non-protein-coding transcripts, designated long non-coding RNAs (lncRNAs), which are transcribed from a large proportion of the human genome [7,8]. Through their regulation of gene expression, lncRNAs have crucial roles in many processes, including development, differentiation, and carcinogenesis [9,10]. Expression of lncRNAs is frequently dysregulated in cancer, and specific lncRNAs correlate with

cancer recurrence, metastasis, and a poor prognosis in various cancer types [11,12]. As a consequence, several lncRNAs, such as MALAT1, HOTAIR, PVT1, and lncRNA-p21, have been identified to play significant roles in cancer initiation and development [9,13–15].

In this study, we aimed to identify and characterize lncRNAs with functional impacts on PC. Cytoplasmic Linc01060 was significantly decreased in PC cell lines compared with HPDE cells. We also found that Linc01060 expression regulates the invasion and metastasis of PC cells *in vitro* and *in vivo*. *In situ* hybridization (ISH) and quantitative real-time polymerase chain reaction (qRT-PCR) analyses revealed that Linc01060 expression decreased significantly in PC tissues, whereas Linc01060 expression correlated directly with patient survival. Linc01060 overexpression suppressed PC cell invasion and metastasis by inhibiting vinculin and upregulating FAK Y-397 and paxillin Y-118, thereby promoting focal adhesion turnover and enhancing cell motility. In conclusion, Linc01060 represses PC invasion and metastasis by inhibiting vinculin-mediated focal adhesion turnover. These provide new insights into the significance of lncRNAs in PC and implicate Linc01060

* Corresponding author. 1095 Jiefang Ave, Wuhan City, Hubei Province, 430030, People's Republic of China.

** Corresponding author. 1095 Jiefang Ave, Wuhan City, Hubei Province, 430030, People's Republic of China.

*** Corresponding author. 1095 Jiefang Ave, Wuhan City, Hubei Province, 430030, People's Republic of China.

E-mail addresses: 2013j0574@hust.edu.cn (X. Li), minwang@tjh.tjmu.edu.cn (M. Wang), ryqin@tjh.tjmu.edu.cn (R. Qin).

¹ These authors contributed equally to this work.

in the progression of PC.

2. Material and methods

2.1. Patient cohort and selection of candidate lncRNAs

To identify the differentially expressed lncRNAs in PC, we screened the lncRNAs in the GEO database. As a result, we obtained expression data from 51 PC tissues and 37 pancreatic tissues from seven human microarray datasets: GSE86436 (Liu et al., 2016), GSE101094 (Shao et al., 2016), GSE57144 (Li et al., 2014), GSE89139 (Zhou et al., 2016), GSE18490 (Miya et al., 2013), GSE71533 (Sandhu et al., 2017), and GSE61166 (Chen et al., 2014). The microarray probes were reannotated to lncRNAs, and the R package limma was used to calculate the levels of the differentially expressed lncRNAs.

2.2. Cell culture

Human PC cell lines (PANC-1, MIA-PaCa-2, ASPC-1, SW1990, BXPC-3, CFPAC-1, Panc 03.27) and the normal pancreatic duct epithelial cell line HPDE were purchased from ATCC (Manassas, VA, USA) and authenticated by STR typing. PANC-1 cells were cultured in Dulbecco's Modified Eagle's Medium (DMEM), containing fetal bovine serum (FBS) at a final concentration of 10%. MIA PaCa-2 cells were cultured in DMEM medium, with FBS concentration of 10% and horse serum at a concentration of 2.5%. ASPC-1 and BXPC-3 cells were cultured in RPMI-1640 Medium, with FBS concentration of 10%. Panc 03.27 were cultured in RPMI-1640 Medium, with FBS concentration of 10% and 10 units/ml human recombinant insulin. SW1990 cells were cultured in Leibovitz's L-15 Medium, with FBS concentration of 10%. CFPAC-1 cells were cultured in Iscove's Modified Dulbecco's Medium, with FBS concentration of 10%. HPDE cells were cultured in 75% DMEM without glucose and 25% Medium M3 Base, with FBS concentration of 5%, 10 ng/ml human recombinant EGF, 5.5 Mm d-glucose (1 g/L) and 750 ng/ml puromycin. All cell lines were cultured at 37 °C in a humidified atmosphere containing 5% CO₂. For RNA stability assays, the cells were treated with 5 mg/ml actinomycin D or 10 mM triptolide (Sigma) at specified time points.

2.3. Patients and samples

PC tissues and matching adjacent normal pancreatic tissues were obtained from 90 patients who underwent surgery at Tongji Hospital (Wuhan, China) between January 2010 and November 2017. None had received any preoperative treatment. All samples were processed by two professional pathologists. The fresh tissue specimens were snap-frozen in liquid nitrogen and stored at -80 °C until RNA isolation. This study was approved by the Human Ethics Committee of Tongji Hospital, Huazhong University of Science and Technology (Wuhan, China) and carried out in accordance with the Declaration of Helsinki.

2.4. RNA microarrays

Total RNA was extracted from si-Linc01060 and NC samples using the Agilent RNA 6000 Nano Kit (Waltham, MA USA) and subjected to microarray analysis with a PrimeView Human GeneChip (Affymetrix, Waltham, MA USA). RNA labeling and hybridization to the microarray chip were performed with the GeneChip Hybridization Wash and Stain Kit (Affymetrix).

2.5. RNA ISH and FISH

RNA ISH experiments were performed with the RNA ISH Kit (BersinBi, Beijing, China) according to the manufacturer's instructions. Briefly, PC cells were fixed in 4% paraformaldehyde for 20 min, washed with distilled water, treated with pepsin (1% in 10 mM HCl), and

incubated with 20 nM ISH probe in hybridization buffer (100 mg/mL dextran sulfate, 10% formamide in 2X SSC) at 90 °C for 3 min. Hybridization was performed at 37 °C for 18 h, followed by a wash step and an incubation with digoxin antibodies for 1 h. Finally, DAB was applied to the samples to detect the signals.

The ISH images were captured using an Aperio ImageScope system. Each sample was examined by two pathology specialists who were blinded to the diagnoses and outcomes. Staining intensities and percentages of positive cells were recorded. The relative expression of each sample was calculated as the product of the expression intensity and percentage of positivity. For FISH, the LNA probe signals were determined using a tyramide signal amplification (PerkinElmer, USA) system. In brief, the signal was detected by incubation with horseradish peroxidase (HRP)-conjugated anti-DIG. Then, the signals were amplified using tetramethylrhodamine (TRITC)-conjugated tyramide. The images were acquired under a fluorescence microscope.

2.6. RNA immunoprecipitation

PANC-1 cells were co-transfected with pcDNA3.1-MS2, pcDNA3.1-MS2-Linc01060, pcDNA3.1-MS2-Linc01060-Mut and pMS2-GFP (Addgene). After 48 h, cells were used to perform RNA immunoprecipitation (RIP) experiments using a GFP antibody (Sigma) and the Imprint[®]RNA Immunoprecipitation (RIP) Kit (Sigma) according to the manufacturer's instructions. The RNA in the RIP material was detected by qRT-PCR analysis.

2.7. Animal experiments

All animal experiments were approved by the Committee on Ethics of Animal Experiments of Huazhong University of Science and Technology (Permit No. 2016-S014), and all treatments were carried out according to the US Public Health Service Policy on the Humane Care and Use of Laboratory Animals. All surgeries were conducted under anesthesia with sodium pentobarbital. For the tumorigenicity assays, PANC-1 and MIA PaCa-2 cells (2×10^6 cells in 100 μ L DMEM without FBS) were injected subcutaneously into the upper right flank of nude mice (4–6-week-old female Balb/c/nu mice). Tumor sizes were measured with a Vernier caliper every 3 days. For the metastasis assays, PANC-1 and MIA PaCa-2 cells (2×10^6 cells in 100 μ L DMEM without FBS) were injected into the spleens of nude mice. All *in vivo* experiments were performed under specific pathogen-free conditions. Mice were euthanized at 8 weeks after inoculation, and their tumor tissues were harvested, weighed, imaged, embedded in 10% paraffin, and subjected to IHC staining.

2.8. Statistical analyses

The results for continuous variables are presented as mean \pm SD unless otherwise stated. Treatment groups were compared by independent-sample *t*-test. Pairwise multiple comparisons were performed by one-way ANOVA (two-sided). $p < 0.05$ was considered to be statistically significant. All analyses were performed using SPSS, version 21.0 (SPSS Inc., IL, USA).

More detailed materials and methods can be found in the [Supplementary Materials and Methods](#) online.

3. Results

3.1. Dysregulation of Linc01060 in PC tissues is significantly associated with a poor prognosis

We initially screened for differentially expressed lncRNAs in PC tissues compared with normal pancreatic tissues. We selected 349 lncRNAs that were differentially expressed, 243 of which were downregulated and 106 were upregulated; an overview of the aberrantly

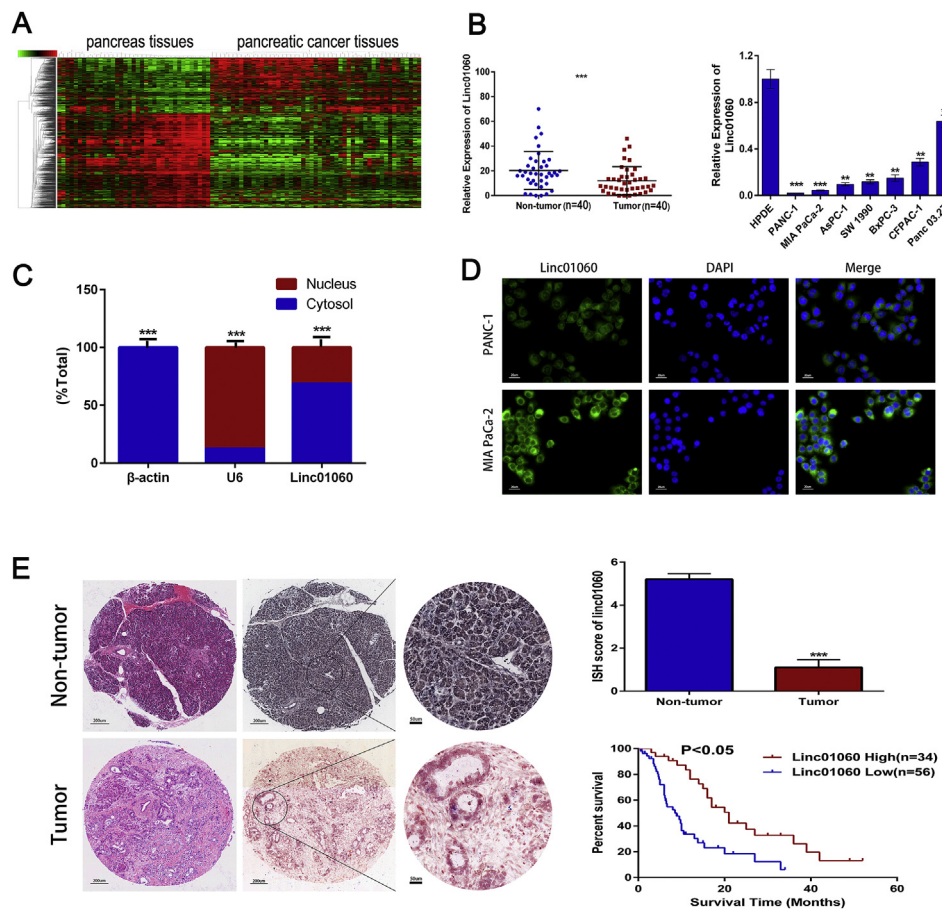


Fig. 1. Aberrant expression of Linc01060 in PC tissues. (A) Cluster analysis of lncRNAs in pancreatic tissues from PC patients and normal pancreatic tissues. (B) Expression of Linc01060 in PC tissues and PC cells analyzed by PCR, ** $p < 0.01$, *** $p < 0.001$. (C) PCR analysis of RNA purified from nuclear (red) and cytosolic (blue) compartments of PANC-1 cells. (D) Detection of endogenous Linc01060 expression in PC cells by FISH. (E) HE and ISH of Linc01060 expression in paraffin-embedded PC specimens and adjacent non-tumor tissues. (F) Patients were divided into those with Linc01060 expression above (Linc01060-high) and below (Linc01060-low) the average value. Kaplan-Meier analysis of the OS of patients. (For interpretation of the references to colour in this figure legend, the reader is referred to the Web version of this article.)

expressed lncRNAs is provided in Fig. 1A. Among the selected lncRNAs, Linc01060 showed the lowest expression in PC versus normal pancreatic tissues.

Linc01060 does not contain the Kozak consensus sequence, which is required for efficient translation [16]. Next, we used PhyloCSF from UCSC to calculate its coding potential [17]. The PhyloCSF score of Linc01060 was lower than 0, supporting that Linc01060 has no protein-coding potential. The Coding Potential Calculator was used to confirm that Linc01060 has no protein-coding potential (score = -1.19299) [18].

Linc01060 underwent the most extensive downregulation in PC tissues and PC cell lines (Fig. 1B). Thus, we hypothesized that Linc01060 plays an important role in PC. According to cytoplasmic/nuclear RNA fractionation and FISH analysis of PC cells, Linc01060 expression was high in the cytoplasm (Fig. 1C and D). Linc01060 expression was then measured in 90 pairs of paraffin-embedded PC surgical specimens by ISH at Tongji Hospital.

Linc01060 was significantly downregulated in PC versus adjacent normal tissues ($p < 0.001$; Fig. 1E). Notably, patients with higher tissue Linc01060 levels ($n = 34$; median survival: 21 months) had slightly longer overall survival (OS) than those with lower levels ($n = 56$; median survival: 10 months; Fig. 1E). Furthermore, Linc01060 overexpression correlated significantly with tumor size, lymph node metastasis, and tumor stage (Supplementary Table 1). No significant link was observed between Linc01060 overexpression and age or sex.

3.2. Linc01060 inhibits PC cell proliferation in vitro and in vivo

To determine the significance of Linc01060 in PC, we performed gain-of-function and loss-of-function studies *in vitro* and *in vivo*. Stable Linc01060-upregulated (Linc01060U) and Linc01060 knockdown

(Linc01060KD) PC cell lines were established using a lentiviral delivery system (Fig. 2A). CCK-8 proliferation assay and colony formation assay showed that Linc01060U PC cells experienced significantly impaired growth and formed fewer colonies compared with negative control (NC) cells (Fig. 2B and C). Linc01060KD PC cells grew faster than NC cells.

For the *in vivo* studies, we generated a xenograft tumor model by subcutaneously injecting Linc01060U, Linc01060KD, and NC cells into the flanks of nude mice. Linc01060 overexpression decreased the tumor growth rate and mean tumor volume markedly compared with the NC group, whereas Linc01060 knockdown had the opposite results (Fig. 2D). The average Linc01060 expression level in xenograft tumors was higher in the Linc01060U versus NC group but lower in the Linc01060KD compared with NC group.

IHC staining was performed on paraffin-embedded samples of xenograft tumors from the Linc01060U, Linc01060KD, and NC groups. Ki-67 and PCNA expression was higher in the xenograft tumors of the Linc01060KD versus NC group but lower in those of the Linc01060U compared with NC group (Fig. 2E).

3.3. Linc01060 inhibits PC cell invasion and metastasis *in vitro* and *in vivo*

Transwell and scratch wound-healing assays showed that the upregulation of Linc01060 reduced PANC-1 and MIA-PaCa-2 cell invasion compared with control cells, whereas Linc01060 knockdown promoted PC cell invasion and metastasis (Fig. 3A and B, Supplementary Fig. 1, Supplementary Fig. 2). For the *in vivo* studies, we generated a spleen xenograft tumor model by injecting PC cells into the spleens of nude mice and counted the number of metastatic tumor nodules in the liver on stable Linc01060 overexpression or Linc01060 knockdown. Linc01060U cells showed less live colonization compared with the NC

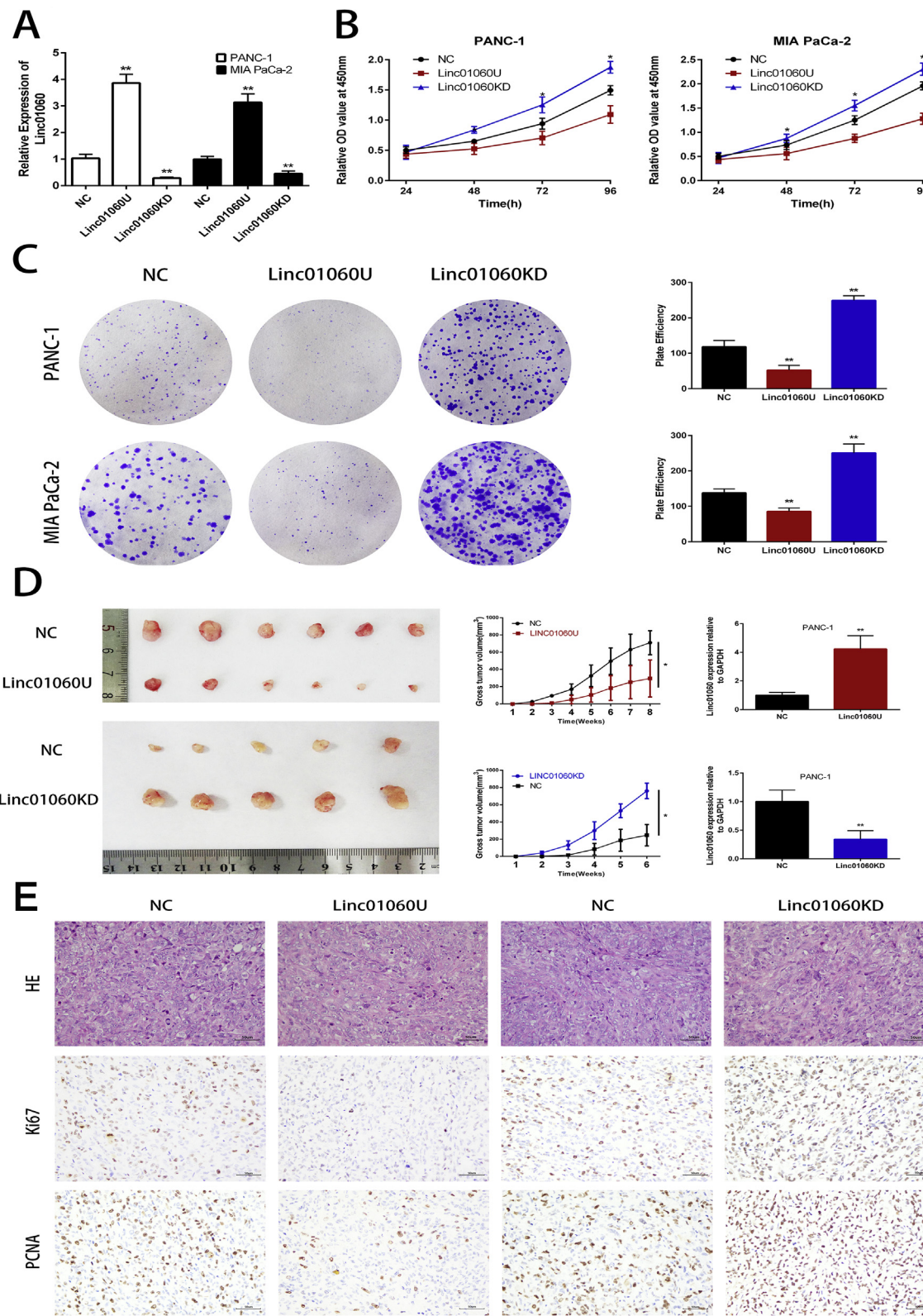


Fig. 2. Linc01060 suppresses the proliferation of PC cells *in vitro* and *in vivo*. (A) Linc01060 expression in PANC-1 and MIA PaCa-2 cells infected with lentiviruses carrying Linc01060-knockdown (Linc01060KD), Linc01060-overexpression (Linc01060U), and negative control (NC) shRNAs analyzed by PCR. (B) CCK-8 assay comparing the proliferation of Linc01060KD, Linc01060U, and NC PANC-1 and MIA-PaCa-2 cells. * $p < 0.05$. (C) Representative images of colony formation assay (left panels) and analysis of colony numbers (right panels). All experiments were performed in triplicate, and data are presented as mean \pm SD. ** $p < 0.01$. (D) Representative images of tumors forming in nude mice ($n = 6$, left panel), mouse tumor volume growth curves for subcutaneous xenografts (middle panel), and Linc01060 expression in xenograft tumors harvested from nude mice analyzed by PCR (right panel). (E) Representative images of IHC staining showing Ki-67 and PCNA expression in xenograft tumor tissues from the various experimental mouse groups.

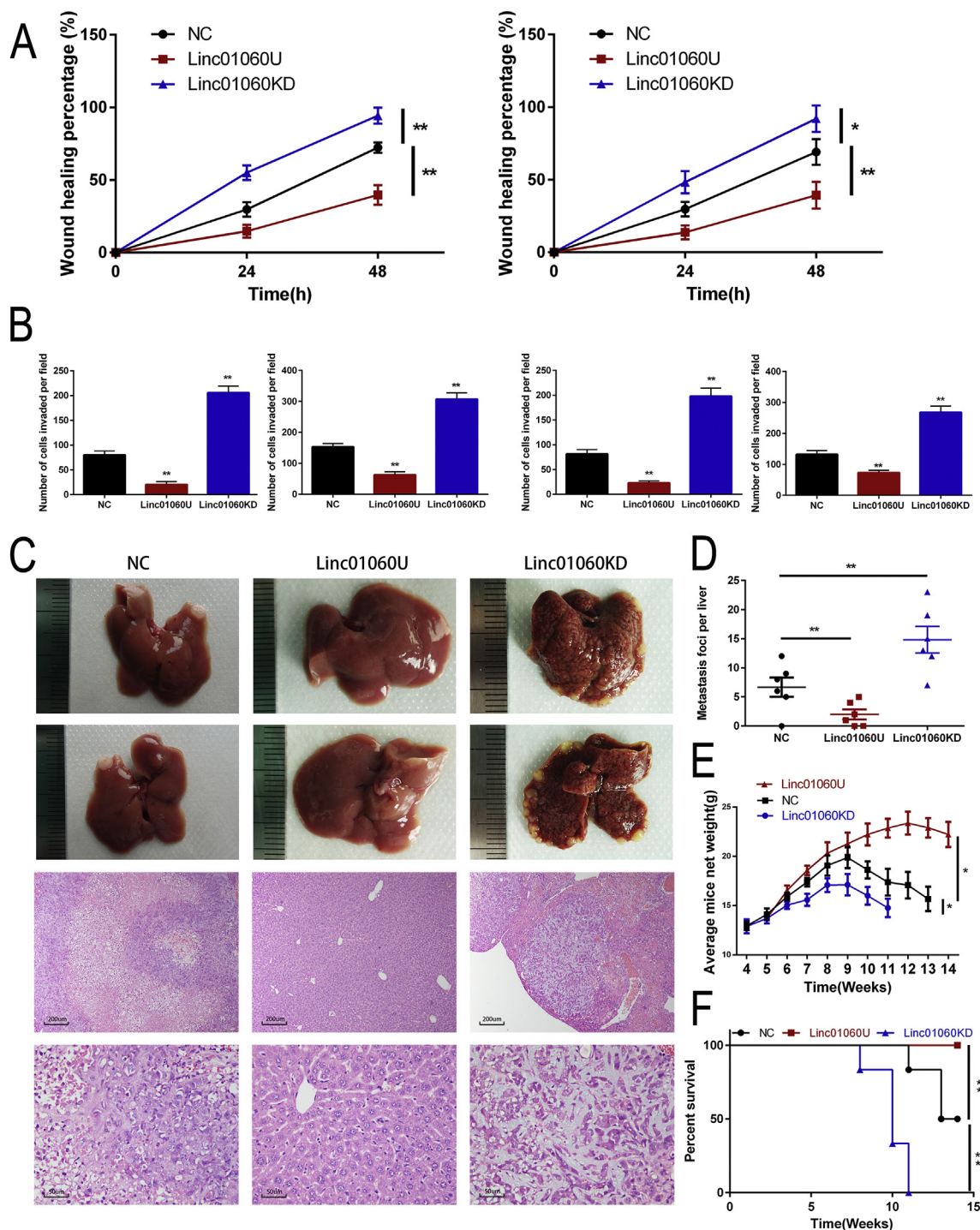


Fig. 3. Linc01060 suppresses the migration and invasion of PC cells *in vitro* and *in vivo*. (A) Wound-healing percentages analyzed using Image-pro plus 6.0. All experiments were performed in triplicate, and data are presented as mean \pm SD. * p < 0.05, ** p < 0.01. (B) Invasion and migration of the indicated cell lines evaluated by Transwell assay. All experiments were performed in triplicate, and data are presented as mean \pm SD. ** p < 0.01. (C) Images from the liver metastasis model. (D) Changes in mouse weight in the PANC-1 Linc01060U and PANC-1 Linc01060KD groups versus the NC group. (E) Kaplan-Meier survival curves for the various experimental mouse groups (NC, Linc01060U, and Linc01060KD; n = 6 mice per group). (F) Statistical analysis of the average numbers of visible liver metastases. Data are presented as mean \pm SD, with each data point representing a different mouse (n = 6 mice per group). * p < 0.05, ** p < 0.01, *** p < 0.001 by student's *t*-test.

group, whereas Linc01060KD cells underwent greater colonization (Fig. 3C and D). The Linc01060KD group experienced more rapid weight loss versus the Linc01060U and NC groups (Fig. 3E).

In the survival analyses, the Linc01060U group had the longest survival time, and Linc01060KD had the shortest survival (Fig. 3F). Our studies confirm that Linc01060 inhibits PC cell proliferation and

invasion, suggesting that Linc01060 is critical in suppressing the development of PC.

3.4. Linc01060 affects focal adhesion turnover and the cell cycle

To examine the processes that are affected by Linc01060, were

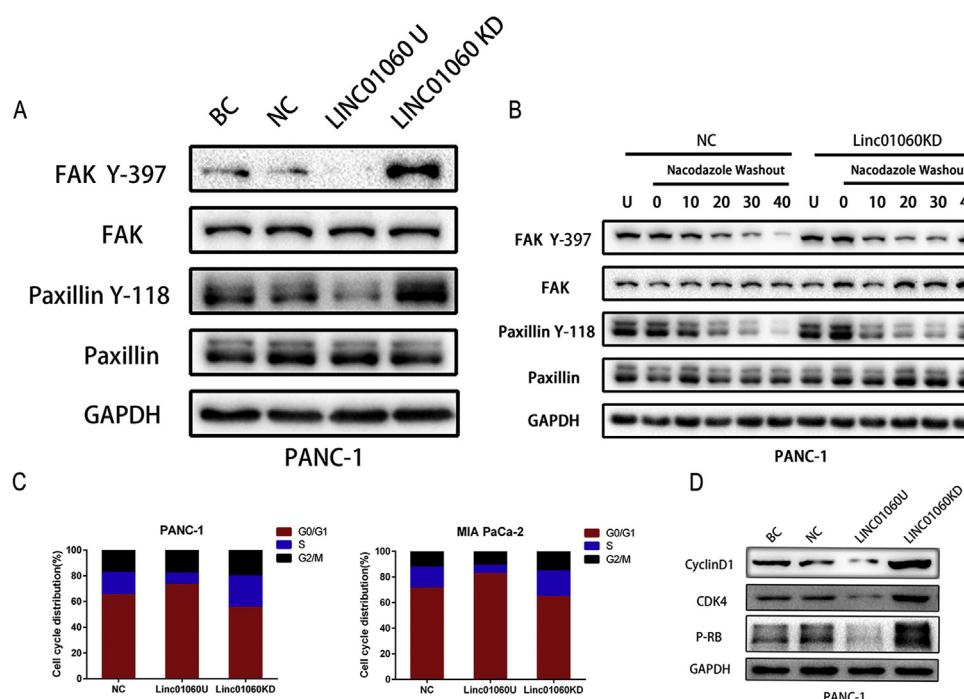


Fig. 4. Linc01060 affects focal adhesion turnover. (A) Western blot analysis showing focal adhesion protein expression in blank control (BC), negative control (NC), Linc01060-overexpression (Linc01060U), and Linc01060-knockdown (Linc01060KD) PANC-1 cells. (B) Representative western blotting of focal adhesion disassembly assay. PANC-1 cells were incubated with 10 mM nocodazole, followed by drug washout and microtubule regrowth. Linc01060KD cells showed more rapid recovery of pFAK Y-397 and pPaxillin Y-118 compared with control cells. (C) Effects of Linc01060 overexpression and Linc01060 knockdown on cell cycle progression in PANC-1 and MIA PaCa-2 cells (left panel), and western blot analyses of cell cycle protein expression in Linc01060U, Linc01060KD, BC, and NC PANC-1 cells (right panel).

performed mRNA microarray analyses in PANC-1 cells at 36 h after transfection with a Linc01060 or negative control siRNA. Using gene ontology analysis, we observed significant enrichment of genes involved that regulate focal adhesions and the cell cycle (Supplementary Fig. 3). Focal adhesions are critical signaling and structural hubs in migrating cells that assemble in response to interactions with extracellular matrix (ECM) ligands.

We confirmed the changes in focal adhesions by western blot analyses of PC cells. Linc01060 knockdown increased FAK and paxillin phosphorylation, whereas Linc01060 overexpression inhibited it (Fig. 4A), suggesting that Linc01060 affects focal adhesion turnover in PC cells.

To test this hypothesis, we performed a nocodazole-based assay. Treatment of cells with nocodazole, a microtubule-disrupting agent, inhibits microtubule targeting and disassembly of the focal adhesion complex. After nocodazole is washed out, microtubule targeting of focal complexes occurs and promotes focal complex turnover and cell spreading. Notably, Linc01060KD cells showed more rapid loss of FAK and paxillin phosphorylation than control cells (Fig. 4B). According to flow cytometry, Linc01060 overexpression resulted in a substantial accumulation of PC cells in G0/G1 phase, which was accompanied by a significant decrease in PC cells in S phase. In contrast, Linc01060 knockdown effected a severe decrease in PC cells in G0/G1 phase but a rise in S-phase PC cells (Fig. 4C). In western blot analysis, Linc01060 overexpression downregulated cyclin D1, CDK4, and p-RB—all of which promote cell cycle progression—whereas Linc01060 knockdown arrest cell cycle progression (Fig. 4D).

3.5. Vinculin is a key downstream target of Linc01060

Because the microarray analyses indicated that Linc01060 significantly affects focal adhesions, we examined genes that are involved in focal adhesion-related signaling that might be affected by Linc01060 (Supplementary Fig. 4). We verified the results by real-time PCR and identified genes that were regulated by Linc01060 (Supplementary Fig. 5). Of the 8 genes, only 4 met the criteria for cis-regulation by Linc01060 (Fig. 5A). An RNA-RNA interaction site was computationally predicted to span Linc01060 and vinculin mRNA (Fig. 5B). Linc01060 knockdown lowered vinculin levels (Fig. 5C), and Linc01060

overexpression significantly upregulated vinculin (Fig. 5D).

To identify the region in Linc01060 that stabilizes vinculin mRNA, we overexpressed a panel of Linc01060 mutants and measured the stability of vinculin mRNA following treatment with triptolide. As expected, Linc01060 overexpression promoted vinculin mRNA stability (Fig. 5E).

To validate the direct binding between vinculin and Linc01060 at endogenous levels, we performed RNA immunoprecipitation (RIP) to pull down endogenous mRNAs that associated with Linc01060. qPCR showed that the immunoprecipitate with Linc01060 in Panc-1 cells was significantly enriched for vinculin compared with empty vector (MS2), IgG, and Linc01060 with mutations in the vinculin targeting sites (Fig. 5F). The specific association between vinculin mRNA and Linc01060 was validated by affinity pull-down of endogenous vinculin mRNA using in vitro-transcribed biotin-labeled Linc01060 (Fig. 5F).

3.6. Linc01060 represses the progression of PC by upregulating vinculin to affect focal adhesion turnover and activating ERK

Unlike FAK, Src, and Cas, vinculin impedes focal adhesion turnover and impairs cell motility [19]. Thus, we hypothesized that Linc01060 represses PC invasion and metastasis by upregulating vinculin. To test this hypothesis, we examined the ability of vinculin to overcome the Linc01060-mediated activation of focal adhesion turnover in PC cells.

Western blot analyses showed that vinculin overexpression inhibited the Linc01060-mediated increases in FAK and paxillin phosphorylation, whereas vinculin knockdown reversed the Linc01060KD-mediated repression of this phosphorylation and inactivated focal adhesion turnover (Fig. 6A and B). Biological function analyses showed that vinculin overexpression abrogated the Linc01060-mediated repression of the progression of PC, whereas vinculin knockdown promoted Linc01060-mediated repression of PC progression (Fig. 6C and D). In our western blot analyses, vinculin overexpression inhibited the Linc01060-mediated increases in p-ERK, and vinculin knockdown reversed the Linc01060KD-mediated repression of p-ERK and prevented progression of the cell cycle (Fig. 6E). Our data demonstrate that Linc01060 has a key role in suppressing PC invasion and metastasis by regulating vinculin expression, implicating the Linc01060-vinculin-focal adhesion axis as a therapeutic target for the treatment of PC

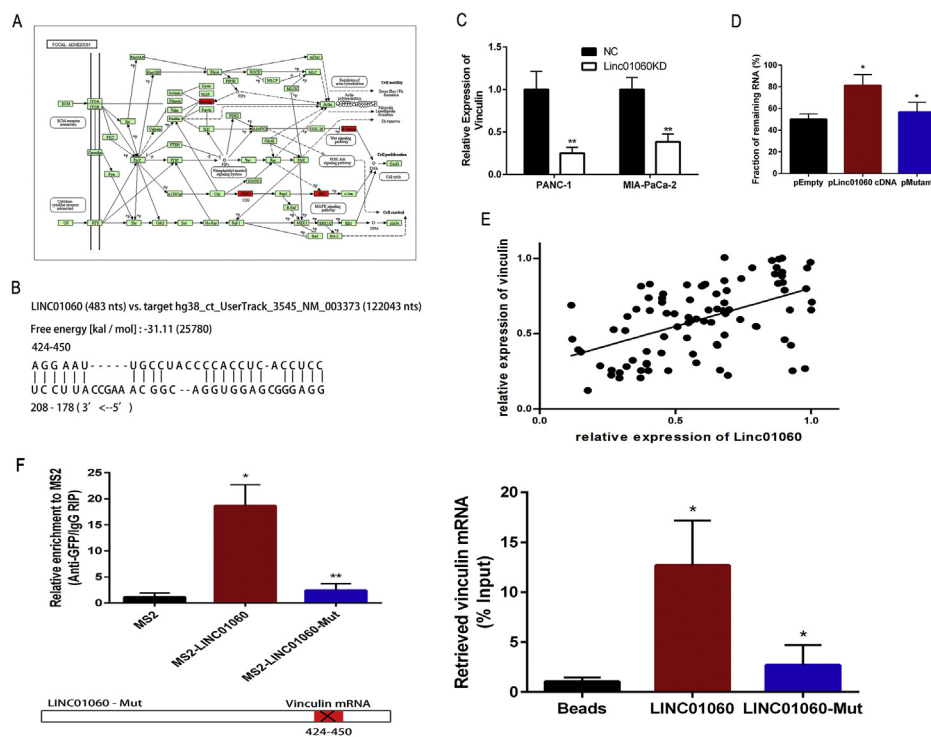


Fig. 5. Vinculin is a key downstream target of Linc01060. (A) Annotation of focal adhesion-related genes that could be regulated by Linc01060, as validated by microarray and PCR analyses, and cis-regulated by Linc01060. (B) Interaction site between Linc01060 and vinculin mRNA predicted by computation. (C) Relative expression of vinculin mRNA between the si-Linc01060 and NC groups of PANC-1 and MIA PaCa-2 cells. (D) PANC-1 cells (2×10^5) were transfected with the indicated plasmids. At 48 h after transfection, the cells were treated with triptolide (final concentration: 10 nM) for 8 h and processed for RNA isolation. The percentage of vinculin mRNA was normalized to the corresponding expression levels in untreated cells. (E) Linear relationship between Linc01060 and vinculin expression in PC tissues ($p < 0.05$). (F) MS2-RIP followed by vinculin mRNA qRT-PCR to detect vinculin mRNAs endogenously associated with Linc01060. PANC-1 cell lysates were incubated with biotin-labeled Linc01060; after pull-down, vinculin mRNA was extracted and assessed by qRT-PCR.

(Fig. 7). These findings suggest that Linc01060 regulates the dynamics of focal adhesions.

4. Discussion

PC remains one of the most aggressive human cancers [20,21]. Despite substantial efforts, PC is associated with a short survival period, which has been steadily declining since the early 1990s [22–24]. There is an urgent need to increase our understanding of the underlying mechanism [25–27]. Recent research has advanced our understanding of the essential role of lncRNAs in PC [28–31]. Although thousands of lncRNAs have been functionally characterized, most members of this RNA class have not been thoroughly described.

Using qRT-PCR, we showed that Linc01060 levels were reduced in PC tissue samples and PC cell lines, suggesting that decreased Linc01060 expression is a promising marker for PC. In addition, ISH analyses showed that Linc01060 expression was significantly down-regulated in 90 paired paraffin-embedded PC specimens and that decreased Linc01060 expression correlated with poor survival in PC patients.

Cancer is fundamentally a genetic disease with numerous alterations in DNA, RNA, and proteins that support tumor growth and development [32–34]. The molecular and cellular characteristics of cancer-associated lncRNAs are under distinct regulatory regimes that differ from physiological conditions [35–37]. In our study, we performed gain-of-function and loss-of-function studies *in vitro* and *in vivo* to demonstrate that Linc01060 plays a critical role in the inhibition of cell proliferation, invasion, and metastasis in PC.

Cell migration occurs during embryonic development, wound healing, immune surveillance, and cancer metastasis and involves dozens of molecular factors [38–42]. The formation and turnover of focal adhesions are essential for cell migration. Focal adhesions are critical signaling and structural hubs in migrating cells that assemble in response to interactions between ECM ligands and integrin receptors [43]. Engagement of integrin with the ECM stimulates tyrosine phosphorylation of key cytoskeletal proteins, beginning with the autophasphorylation of Y397 in FAK [44].

FAK autophasphorylation recruits Src to focal adhesions, and the

resulting FAK/src complexes phosphorylate two adapter proteins, paxillin and p130CAS [45]. Phosphorylated paxillin and p130CAS recruit proteins, such as Crk, to focal adhesions through SH2/S3-binding domains. Fibroblasts that are deficient in FAK or paxillin exhibit defects in cell migration, suggesting that Src-mediated tyrosine phosphorylation of FAK and paxillin and the assembly of FAK/paxillin signaling complexes are key events that regulate focal adhesion dynamics and cell motility [46,47]. However, the mechanism by which lncRNAs regulate focal adhesions in PC remains unknown.

In this study, according to western blot analyses of PC cells, Linc01060 knockdown upregulated FAK Y-397 and paxillin Y-118, whereas Linc01060 overexpression inhibited it. Immunofluorescence analyses also showed that Linc01060 knockdown increased focal adhesion turnover. It remains unknown whether Linc01060 regulates PC metastasis by affecting focal adhesion turnover.

Vinculin is a ubiquitous, highly conserved cytoskeletal protein that is localized at cell-cell and cell-ECM junctions [48]. It can form part of a complex that couples members of the cadherin and integrin families of cell adhesion molecules to the actin cytoskeleton, although the identification of growing numbers of binding partners and modes of regulation suggests that vinculin is not merely a simple linker protein. Studies in vinculin-null cells have established that it is not required for assembly of integrin-containing cell-ECM junctions (focal adhesions) or cadherin-containing cell-cell junctions in cultured cells, although it is essential for tight junction assembly [49,50]. Instead, vinculin-null cells show less spreading, have fewer focal adhesions, and are more motile in Transwell assays, indicating a role for vinculin in the negative regulation of cell motility.

Our microarray and qRT-PCR analyses indicated that Linc01060 knockdown significantly affects vinculin mRNA levels. Using a bioinformatics prediction tool, we identified a potential RNA-RNA interaction site between Linc01060 and vinculin mRNA. Recently, many lncRNAs have been reported to interact with mRNAs and increase mRNA stability [51,52]. We therefore assessed the ability of vinculin to overcome the Linc01060-mediated activation of focal adhesion turnover in PC cells. Western blotting analyses showed that vinculin overexpression inhibited the Linc01060-mediated increases in FAK and paxillin phosphorylation, whereas vinculin knockdown reversed the

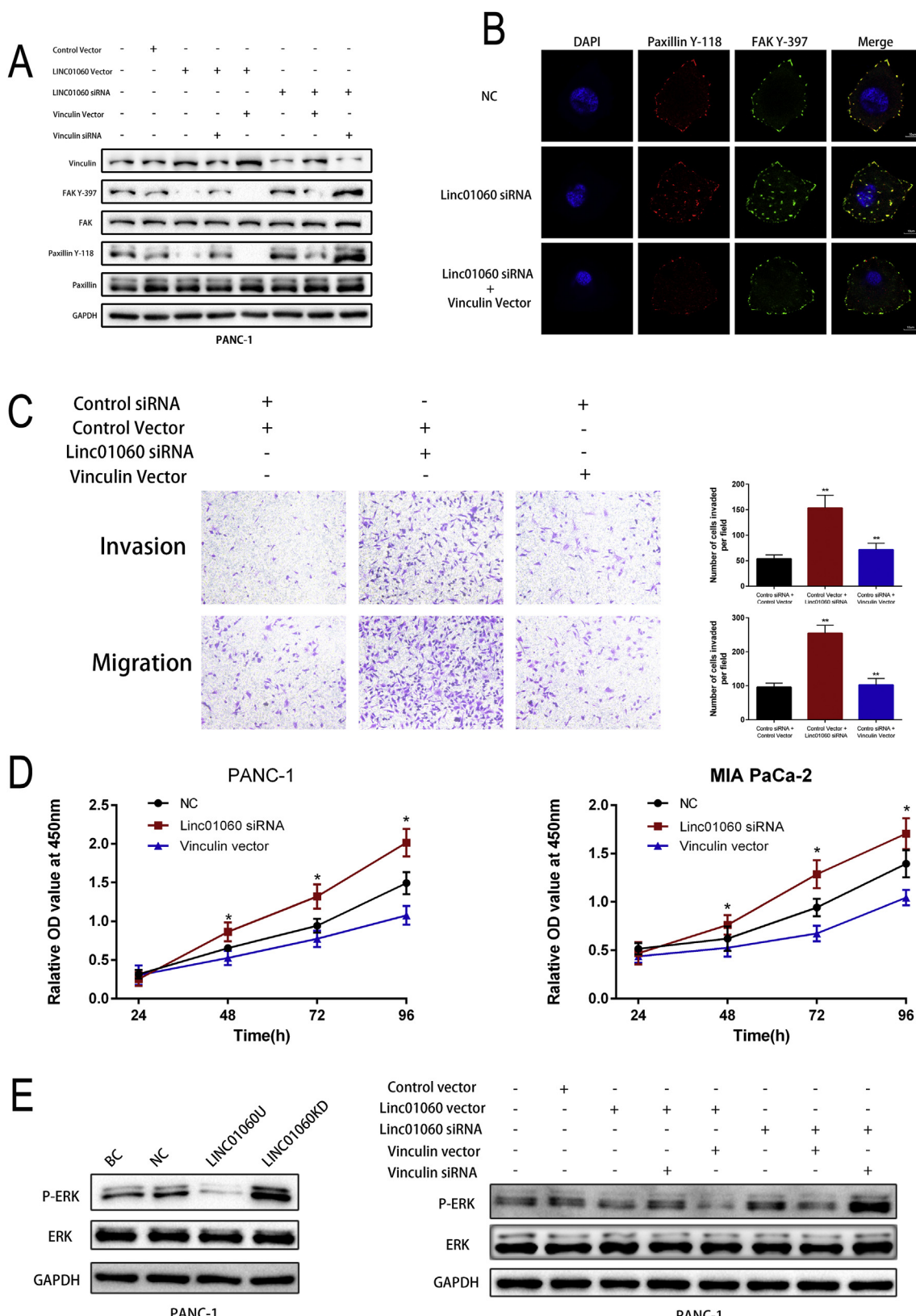


Fig. 6. Linc01060 represses PC progression via the Linc01060-vinculin-focal adhesion axis. (A) Western blot analysis of the protein expression levels of key modulators of the focal adhesion signaling pathway in PANC-1 cells transfected with various plasmids. (B) Immunofluorescent staining of cells for focal adhesion markers (phospho-FAK-397 and phospho-paxillin-118). Scale bar, 20 nm. (C) Transwell assay showing that vinculin overexpression abrogates the si-Linc01060-mediated promotion of PC cell invasion. (D) CCK-8 assay comparing the proliferation of PANC-1 and MIA-PaCa-2 cells transfected with Linc01060 siRNA, vinculin vector, and NC siRNA. (E) Western blot analysis of ERK and p-ERK expression in Linc01060U, Linc01060KD, blank control (BC), and NC PANC-1 cells. The levels of ERK and p-ERK were analyzed by western blotting in PANC-1 cells transfected with various plasmids. All experiments were performed in triplicate, and data are presented as mean \pm SD. ** p < 0.01.

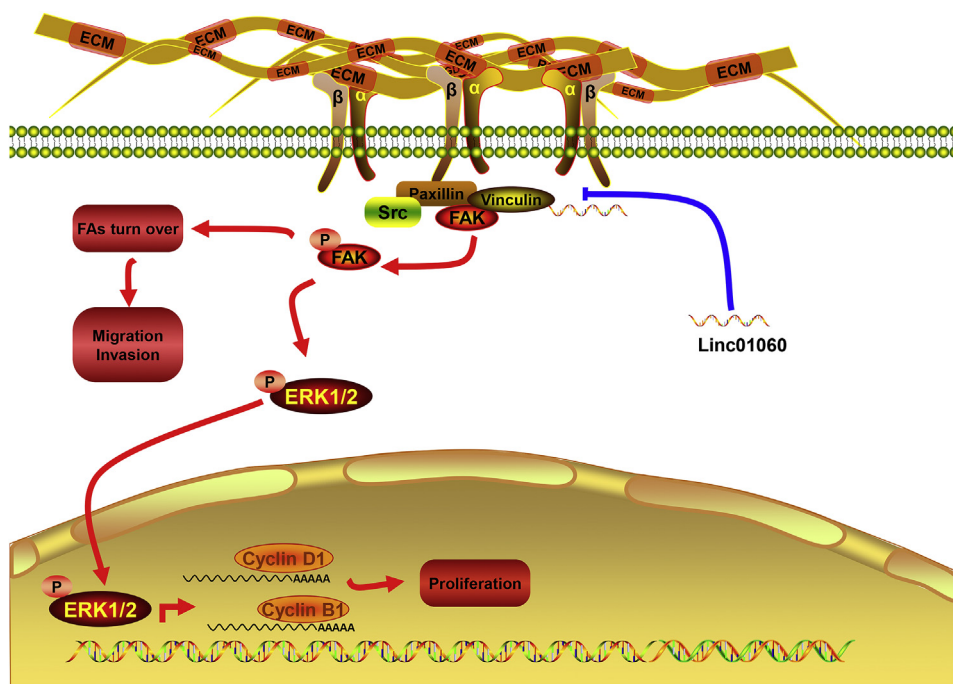


Fig. 7. Schematic of the role of Linc01060 in progression of PC cells.

Linc01060KD-mediated repression of FAK and inactivation of focal adhesion turnover. Our results further showed that vinculin knockdown increases cell proliferation through the upregulation of ERK activity. Biological function analyses showed that vinculin overexpression abrogates the Linc01060-mediated repression of PC cell proliferation and invasion, whereas vinculin knockdown counteracted the Linc01060-mediated repression of PC cell proliferation and invasion.

Our data demonstrate that Linc01060 plays a key role in suppressing PC invasion and metastasis by regulating vinculin expression. These findings suggest that the Linc01060–vinculin–focal adhesion–ERK axis is a therapeutic target for the treatment of PC. This study is the first to investigate the critical role of lncRNAs in the regulation of focal adhesion turnover via vinculin in PC. Thus, targeting Linc01060 is a promising approach for treating PC by inhibiting vinculin and focal adhesion turnover.

Acknowledgments

This study was funded by The National Natural Science Foundation of China (No. 81602475 to X.J.G., No. 81772950 to R.Y.Q., No. 81101621 to M.W., No. 81502633 to X.L.).

Conflicts of interest

The authors declare no conflicts of interest.

Appendix A. Supplementary data

Supplementary data related to this article can be found at <http://dx.doi.org/10.1016/j.canlet.2018.06.015>.

References

- [1] T. Hackert, A. Ulrich, M.W. Buchler, Borderline resectable pancreatic cancer, *Canc. Lett.* 375 (2016) 231–237.
- [2] R.L. Siegel, K.D. Miller, A. Jemal, Cancer statistics, 2016, *CA: Canc. J. Clin.* 66 (2016) 7–30.
- [3] A. Vincent, J. Herman, R. Schulick, R.H. Hruban, M. Goggins, Pancreatic cancer, *Lancet (London, England)* 378 (2011) 607–620.
- [4] A.K. Chaudhary, G. Mondal, V. Kumar, K. Kattel, R.I. Mahato, Chemosensitization and inhibition of pancreatic cancer stem cell proliferation by overexpression of microRNA-205, *Canc. Lett.* 402 (2017) 1–8.
- [5] S.J. Rombouts, J.A. Vogel, H.C. van Santvoort, K.P. van Lienden, R. van Hillegeberg, O.R. Busch, M.G. Besselink, I.Q. Molenaar, Systematic review of innovative ablative therapies for the treatment of locally advanced pancreatic cancer, *Br. J. Surg.* 102 (2015) 182–193.
- [6] G. Luo, C. Liu, M. Guo, J. Long, Z. Liu, Z. Xiao, K. Jin, H. Cheng, Y. Lu, Q. Ni, X. Yu, CA19-9-Low&Lewis (+) pancreatic cancer: a unique subtype, *Canc. Lett.* 385 (2017) 46–50.
- [7] E. Lau, Non-coding RNA: zooming in on lncRNA functions, *Nat. Rev. Genetics* 15 (2014) 574–575.
- [8] P.J. Batista, H.Y. Chang, Long noncoding RNAs: cellular address codes in development and disease, *Cell* 152 (2013) 1298–1307.
- [9] M. Huarte, M. Guttman, D. Feldser, M. Garber, M.J. Koziol, D. Kenzelmann-Broz, A.M. Khalil, O. Zuk, I. Amit, M. Rabani, L.D. Attardi, A. Regev, E.S. Lander, T. Jacks, J.L. Rinn, A large intergenic noncoding RNA induced by p53 mediates global gene repression in the p53 response, *Cell* 142 (2010) 409–419.
- [10] N. Jiang, X. Wang, X. Xie, Y. Liao, N. Liu, J. Liu, N. Miao, J. Shen, T. Peng, lncRNA DANCR promotes tumor progression and cancer stemness features in osteosarcoma by upregulating AXL via miR-33a-5p inhibition, *Canc. Lett.* 405 (2017) 46–55.
- [11] Y. He, X.M. Meng, C. Huang, B.M. Wu, L. Zhang, X.W. Lv, J. Li, Long noncoding RNAs: novel insights into hepatocellular carcinoma, *Canc. Lett.* 344 (2014) 20–27.
- [12] Z. Yang, L. Zhou, L.M. Wu, M.C. Lai, H.Y. Xie, F. Zhang, S.S. Zheng, Overexpression of long non-coding RNA HOTAIR predicts tumor recurrence in hepatocellular carcinoma patients following liver transplantation, *Ann. Surg. Oncol.* 18 (2011) 1243–1250.
- [13] Y.Y. Tseng, B.S. Moriarity, W. Gong, R. Akiyama, A. Tiwari, H. Kawakami, P. Ronning, B. Reuland, K. Guenther, T.C. Beadnell, J. Essig, G.M. Otto, M.G. O'Sullivan, D.A. Largaespada, K.L. Schwertfeger, Y. Marahrens, Y. Kawakami, A. Bagchi, PVT1 dependence in cancer with MYC copy-number increase, *Nature* 512 (2014) 82–86.
- [14] R.A. Gupta, N. Shah, K.C. Wang, J. Kim, H.M. Horlings, D.J. Wong, M.C. Tsai, T. Hung, P. Argani, J.L. Rinn, Y. Wang, P. Brzoska, B. Kong, R. Li, R.B. West, M.J. van de Vijver, S. Sukumar, H.Y. Chang, Long non-coding RNA HOTAIR reprograms chromatin state to promote cancer metastasis, *Nature* 464 (2010) 1071–1076.
- [15] V. Tripathi, J.D. Ellis, Z. Shen, D.Y. Song, Q. Pan, A.T. Watt, S.M. Freier, C.F. Bennett, A. Sharma, P.A. Bubulya, B.J. Blencowe, S.G. Prasanth, K.V. Prasanth, The nuclear-retained noncoding RNA MALAT1 regulates alternative splicing by modulating SR splicing factor phosphorylation, *Mol. Cell* 39 (2010) 925–938.
- [16] M. Kozak, Point mutations define a sequence flanking the AUG initiator codon that modulates translation by eukaryotic ribosomes, *Cell* 44 (1986) 283–292.
- [17] M.F. Lin, I. Jungreis, M. Kellis, PhyloCSF: a comparative genomics method to distinguish protein coding and non-coding regions, *Bioinformatics (Oxford, England)* 27 (2011) i275–i282.
- [18] Y.J. Kang, D.C. Yang, L. Kong, M. Hou, Y.Q. Meng, L. Wei, G. Gao, CPC2: a fast and accurate coding potential calculator based on sequence intrinsic features, *Nucleic Acids Res.* 45 (2017) W12–W16.
- [19] R.M. Saunders, M.R. Holt, L. Jennings, D.H. Sutton, I.L. Barsukov, A. Bobkov, R.C. Liddington, E.A. Adamson, G.A. Dunn, D.R. Critchley, Role of vinculin in

regulating focal adhesion turnover, *Eur. J. Cell Biol.* 85 (2006) 487–500.

[20] R. Siegel, D. Naishadham, A. Jemal, *Cancer statistics, 2013*, CA: *Canc. J. Clin.* 63 (2013) 11–30.

[21] M.J. Kang, J.Y. Jang, S.W. Kim, Surgical resection of pancreatic head cancer: what is the optimal extent of surgery? *Canc. Lett.* 382 (2016) 259–265.

[22] K. Foley, V. Kim, E. Jaffee, L. Zheng, Current progress in immunotherapy for pancreatic cancer, *Canc. Lett.* 381 (2016) 244–251.

[23] J. Kota, J. Hancock, J. Kwon, M. Korc, Pancreatic cancer: stroma and its current and emerging targeted therapies, *Canc. Lett.* 391 (2017) 38–49.

[24] J. Ma, A. Jemal, The rise and fall of cancer mortality in the USA: why does pancreatic cancer not follow the trend? *Future Oncol. (London, England)* 9 (2013) 917–919.

[25] D.M. Fink, M.M. Steele, M.A. Hollingsworth, The lymphatic system and pancreatic cancer, *Canc. Lett.* 381 (2016) 217–236.

[26] B. Hu, K. Zhang, S. Li, H. Li, Z. Yan, L. Huang, J. Wu, X. Han, W. Jiang, T. Muliabieke, L. Zheng, R. Wan, X. Wang, G. Hu, HIC1 attenuates invasion and metastasis by inhibiting the IL-6/STAT3 signalling pathway in human pancreatic cancer, *Canc. Lett.* 376 (2016) 387–398.

[27] S. Midha, S. Chawla, P.K. Garg, Modifiable and non-modifiable risk factors for pancreatic cancer: a review, *Canc. Lett.* 381 (2016) 269–277.

[28] Z. Fu, C. Chen, Q. Zhou, Y. Wang, Y. Zhao, X. Zhao, W. Li, S. Zheng, H. Ye, L. Wang, Z. He, Q. Lin, Z. Li, R. Chen, LncRNA HOTTIP modulates cancer stem cell properties in human pancreatic cancer by regulating HOXA9, *Canc. Lett.* 410 (2017) 68–81.

[29] Q. Wang, J. Zhang, Y. Liu, W. Zhang, J. Zhou, R. Duan, P. Pu, C. Kang, L. Han, A novel cell cycle-associated lncRNA, HOXA11-AS, is transcribed from the 5-prime end of the HOXA transcript and is a biomarker of progression in glioma, *Canc. Lett.* 373 (2016) 251–259.

[30] L. Zhao, H. Kong, H. Sun, Z. Chen, B. Chen, M. Zhou, LncRNA-PVT1 promotes pancreatic cancer cells proliferation and migration through acting as a molecular sponge to regulate miR-448, *J. Cell. Physiol.* 233 (2018) 4044–4055.

[31] H. Cai, J. Yao, Y. An, X. Chen, W. Chen, D. Wu, B. Luo, Y. Yang, Y. Jiang, D. Sun, X. He, LncRNA HOTAIR acts a competing endogenous RNA to control the expression of notch3 via sponging miR-613 in pancreatic cancer, *Oncotarget* 8 (2017) 32905–32917.

[32] D. Hanahan, R.A. Weinberg, Hallmarks of cancer: the next generation, *Cell* 144 (2011) 646–674.

[33] Y. Tang, B.B. Cheung, B. Atmadibrata, G.M. Marshall, M.E. Dinger, P.Y. Liu, T. Liu, The regulatory role of long noncoding RNAs in cancer, *Canc. Lett.* 391 (2017) 12–19.

[34] M.E. Forrest, A.M. Khalil, Review: regulation of the cancer epigenome by long non-coding RNAs, *Canc. Lett.* 407 (2017) 106–112.

[35] G. Xiong, M. Feng, G. Yang, S. Zheng, X. Song, Z. Cao, L. You, L. Zheng, Y. Hu, T. Zhang, Y. Zhao, The underlying mechanisms of non-coding RNAs in the chemoresistance of pancreatic cancer, *Canc. Lett.* 397 (2017) 94–102.

[36] J. Wang, N. Shao, X. Ding, B. Tan, Q. Song, N. Wang, Y. Jia, H. Ling, Y. Cheng, Crosstalk between transforming growth factor-beta signaling pathway and long non-coding RNAs in cancer, *Canc. Lett.* 370 (2016) 296–301.

[37] A.M. Schmitt, H.Y. Chang, Long noncoding RNAs in cancer pathways, *Canc. Cell* 29 (2016) 452–463.

[38] A.J. Ridley, M.A. Schwartz, K. Burridge, R.A. Firtel, M.H. Ginsberg, G. Borisy, J.T. Parsons, A.R. Horwitz, Cell migration: integrating signals from front to back, *Science (New York, N.Y.)* 302 (2003) 1704–1709.

[39] D.A. Lauffenburger, A.F. Horwitz, Cell migration: a physically integrated molecular process, *Cell* 84 (1996) 359–369.

[40] X. Li, C. Ma, L. Zhang, N. Li, X. Zhang, J. He, R. He, M. Shao, J. Wang, L. Kang, C. Han, LncRNAAC132217.4, a KLF8-regulated long non-coding RNA, facilitates oral squamous cell carcinoma metastasis by upregulating IGF2 expression, *Canc. Lett.* 407 (2017) 45–56.

[41] C. Fang, S. Qiu, F. Sun, W. Li, Z. Wang, B. Yue, X. Wu, D. Yan, Long non-coding RNA HNF1A-AS1 mediated repression of miR-34a/SIRT1/p53 feedback loop promotes the metastatic progression of colon cancer by functioning as a competing endogenous RNA, *Canc. Lett.* 410 (2017) 50–62.

[42] K.K. Chan, C.O. Leung, C.C. Wong, D.W. Ho, K.S. Chok, C.L. Lai, I.O. Ng, R.C. Lo, Secretory Stanniocalcin 1 promotes metastasis of hepatocellular carcinoma through activation of JNK signaling pathway, *Canc. Lett.* 403 (2017) 330–338.

[43] A. Huttenlocher, R.R. Sandborg, A.F. Horwitz, Adhesion in cell migration, *Curr. Opin. Cell Biol.* 7 (1995) 697–706.

[44] S.K. Mitra, D.A. Hanson, D.D. Schlaepfer, Focal adhesion kinase: in command and control of cell motility, *Nature reviews, Mol. Cell Biol.* 6 (2005) 56–68.

[45] D.J. Webb, K. Donais, L.A. Whitmore, S.M. Thomas, C.E. Turner, J.T. Parsons, A.F. Horwitz, FAK-Src signalling through paxillin, ERK and MLCK regulates adhesion disassembly, *Nat. Cell Biol.* 6 (2004) 154–161.

[46] C.A. Easley, C.M. Brown, A.F. Horwitz, R.M. Tombes, CaMK-II promotes focal adhesion turnover and cell motility by inducing tyrosine dephosphorylation of FAK and paxillin, *Cell Motil. Cytoskeleton* 65 (2008) 662–674.

[47] M. Hagel, E.L. George, A. Kim, R. Tamimi, S.L. Opitz, C.E. Turner, A. Imamoto, S.M. Thomas, The adaptor protein paxillin is essential for normal development in the mouse and is a critical transducer of fibronectin signaling, *Mol. Cell Biol.* 22 (2002) 901–915.

[48] B.M. Jockusch, M. Rudiger, Crosstalk between cell adhesion molecules: vinculin as a paradigm for regulation by conformation, *Trends Cell Biol.* 6 (1996) 311–315.

[49] W. Xu, J.L. Coll, E.D. Adamson, Rescue of the mutant phenotype by reexpression of full-length vinculin in null F9 cells: effects on cell locomotion by domain deleted vinculin, *J. Cell Sci.* 111 (Pt 11) (1998) 1535–1544.

[50] M. Watabe-Uchida, N. Uchida, Y. Imamura, A. Nagafuchi, K. Fujimoto, T. Uemura, S. Vermeulen, F. van Roy, E.D. Adamson, M. Takeichi, alpha-Catenin-vinculin interaction functions to organize the apical junctional complex in epithelial cells, *J. Cell Biol.* 142 (1998) 847–857.

[51] M.A. Faghihi, F. Modarresi, A.M. Khalil, D.E. Wood, B.G. Sahagan, T.E. Morgan, C.E. Finch, G. St Laurent 3rd, P.J. Kenny, C. Wahlestedt, Expression of a noncoding RNA is elevated in Alzheimer's disease and drives rapid feed-forward regulation of beta-secretase, *Nat. Med.* 14 (2008) 723–730.

[52] J.H. Yoon, K. Abdelmohsen, S. Srikanthan, X. Yang, J.L. Martindale, S. De, M. Huarte, M. Zhan, K.G. Becker, M. Gorospe, LncRNA-p21 suppresses target mRNA translation, *Mol. Cell* 47 (2012) 648–655.